

# Flux creep in $\text{Bi}_2\text{Sr}_2\text{CaCu}_2\text{O}_8$ epitaxial films

E. Zeldov,<sup>a)</sup> N. M. Amer, G. Koren,<sup>b)</sup> and A. Gupta  
 IBM Thomas J. Watson Research Center, Yorktown Heights, New York 10598-0218

(Received 14 December 1989; accepted for publication 26 February 1990)

We incorporate the experimentally deduced flux line potential well structure into the flux creep model. Application of this approach to the resistive transition in  $\text{Bi}_2\text{Sr}_2\text{CaCu}_2\text{O}_8$  epitaxial films explains the power law voltage-current characteristics and the nonlinear current dependence of the activation energy. The results cannot be accounted for by a transition into a superconducting vortex-glass phase.

The power law voltage-current ( $V$ - $I$ ) characteristics in the high  $T_c$  superconductors have been reported extensively.<sup>1-3</sup> Most of this body of work<sup>1</sup> investigates the resistive transition in the absence of or in the presence of very low magnetic fields, and the results are analyzed within the framework of the Kosterlitz-Thouless phase transition.<sup>4</sup> Two recent studies show the existence of power law characteristics in  $\text{YBa}_2\text{Cu}_3\text{O}_7$  epitaxial films in the presence of high magnetic fields.<sup>2,3</sup> Koch *et al.*<sup>2</sup> ascribe this behavior to the transition into a superconducting vortex-glass phase,<sup>5</sup> whereas Zeldov *et al.*<sup>3</sup> attribute it to the shape of the flux line potential well. In this letter we present the results for  $\text{Bi}_2\text{Sr}_2\text{CaCu}_2\text{O}_8$  epitaxial films. We find that the resistive transition and the  $V$ - $I$  characteristics are consistent with the existence of a logarithmically shaped flux line potential well, and cannot be explained by the vortex-glass picture.

The  $\text{Bi}_2\text{Sr}_2\text{CaCu}_2\text{O}_8$  films were laser ablated onto the (100)  $\text{SrTiO}_3$  substrate at 760 °C in the presence of 500 m Torr oxygen pressure.<sup>6</sup> The films were predominantly oriented with  $c$  axis normal to the interface and had critical currents in excess of  $10^6$  A/cm<sup>2</sup> at 20 K. The resistive data were obtained using a dc four-probe technique on microbridge, 18  $\mu\text{m}$  wide, 195  $\mu\text{m}$  long, and 0.6  $\mu\text{m}$  thick, which was patterned by an excimer laser microscope system.<sup>6</sup> A variable magnetic field of up to 6 T was applied parallel to the  $c$  axis and special care was taken to assure the absence of any heating effects in the relevant experimental regions.

Figure 1 shows the Arrhenius plot of the resistive transition of the  $\text{Bi}_2\text{Sr}_2\text{CaCu}_2\text{O}_8$  film in the presence of a magnetic field of 5 T parallel to the  $c$  axis. The resistivity is thermally activated over a wide temperature range and the activation energy is seen to be significantly current dependent at current densities above  $3 \times 10^3$  A/cm<sup>2</sup>. We analyze the results within the framework of the Anderson-Kim flux creep model.<sup>7</sup> The dissipation process is governed by thermally assisted hopping of the flux lines which may be pinned due to some local defects. At low driving forces, the hopping rate is controlled by the height of the potential barrier, regardless of the detailed shape of the potential. In the presence of strong Lorentz force, however, the amount of deformation of the potential well, and hence the resulting barrier height, are determined by the shape of the potential well. We use this

effect as a spectroscopic tool to deduce the shape of the potential well in high  $T_c$  materials.

One of the features of Fig. 1 that necessitates early clarification is the gradual upward bending of the curves, as if the activation energy,  $U(T), \rho(T) = \rho_0 \exp\{-U(T)/kT\}$  decreases with decreasing the temperature. The observed slopes of the Arrhenius curves,  $-kd(\ln \rho)/d(1/T)$ , however, are not the activation energy  $U(T)$ , but rather  $U_{\text{eff}} = U(T) - TdU/dT$ . In fact, the shape of the curves is consistent with the temperature dependence proposed by Tinkham,<sup>8</sup>  $U(t) = U(0)(1-t^2)(1-t^4)^{1/2}$ , analogous to the behavior of  $\text{YBa}_2\text{Cu}_3\text{O}_7$  reported in Ref. 3 ( $t = T/T_c$ ). The theoretical  $U(t)$  gradually increases with decreasing the temperature, reflecting the increase in the condensation energy. Yet, the corresponding  $U_{\text{eff}}$  has a maximum value of  $1.64U(0)$  at  $t = 0.8$  [where  $U(t)$  is only  $0.28U(0)$ ] and then gradually decreases with decreasing the temperature, in qualitative agreement with the experimental curves in Fig. 1.

The main feature of Fig. 1, however, is the nonlinear current dependence of the activation energy. Below  $3 \times 10^3$  A/cm<sup>2</sup>,  $U$  is rather constant and drops logarithmically with current at higher current densities in a manner similar to the results obtained from  $\text{YBa}_2\text{Cu}_3\text{O}_7$  epitaxial films.<sup>3,9</sup> In the latter case, however,  $U(0)$  was on the order of 1 eV at 6 T, whereas in  $\text{Bi}_2\text{Sr}_2\text{CaCu}_2\text{O}_8$  film it is only about 40 meV at 5 T rising to about 120 meV at 0.5 T. Such a large difference in the activation energies of  $\text{YBa}_2\text{Cu}_3\text{O}_7$  and  $\text{Bi}_2\text{Sr}_2\text{CaCu}_2\text{O}_8$  is

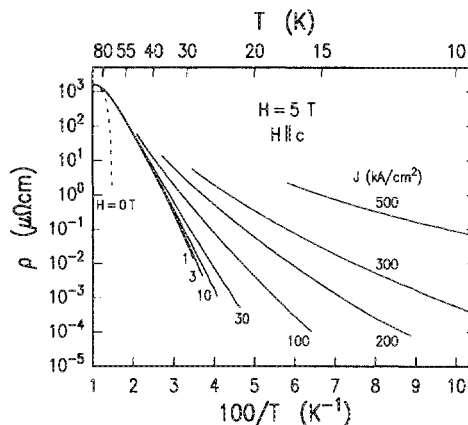


FIG. 1. Arrhenius plot of the resistivity of  $\text{Bi}_2\text{Sr}_2\text{CaCu}_2\text{O}_8$  epitaxial film at  $H = 5$  T and various current densities. For  $J < 3$  kA/cm<sup>2</sup> the measured  $\rho$  is current independent.

<sup>a)</sup> On leave from the Department of Electrical Engineering and Solid State Institute, Technion-Israel Institute of Technology, Haifa 32000, Israel.

<sup>b)</sup> Permanent address: Physics Department, Technion-Israel Institute of Technology, Haifa 32000, Israel.

consistent with the single-crystal magnetic relaxation<sup>10</sup> and transport measurements.<sup>11</sup>

Figure 2 shows the  $\rho$ - $J$  characteristics of the sample at 5 T. Similar behavior is observed at various field intensities, resembling the results for  $\text{YBa}_2\text{Cu}_3\text{O}_7$  films.<sup>3</sup> In the transition region,  $\rho$  is governed by fluctuations and flux flow, with  $\rho$  being current independent (linear  $V$ - $I$  characteristics) down to about 2% of the normal-state resistivity [as compared to 10–15% in  $\text{YBa}_2\text{Cu}_3\text{O}_7$  (Refs. 3, 9, 12)]. At still lower temperatures, flux creep enters as a dominant dissipation mechanism yielding a current independent  $\rho$  at low currents and a nonlinear  $\rho$ - $J$  characteristic at high  $J$  values. However, according to the basic flux creep model,<sup>7</sup> at elevated driving forces, the activation energy is assumed to drop linearly with current and the  $V$ - $I$  characteristics are predicted to be exponential. Instead, we observe a logarithmic  $U(J)$  dependence, and a power law behavior of  $V$  vs  $I$ . We attribute these results as due to the shape of the flux line potential well.

In Ref. 3 it was shown that a potential well which gives rise to the features described above has a logarithmic conical shape. Here we present a more generalized form of this approach. We describe the energy  $V(x)$  of the flux line between the two neighboring wells at locations  $x = 0$  and  $x = L$  as the superposition of their individual contributions. In the presence of a Lorentz force  $F$ ,  $V(x)$  is given by

$$V(x) = \begin{cases} a \left[ \ln \left( \frac{L-x}{L} \right) + \frac{x}{x_0} \right] - Fx & 0 \leq x \leq x_0 \\ a \left[ \ln \left( \frac{x(L-x)}{x_0 L} \right) + 1 \right] - Fx & x_0 < x < L - x_0 \\ a \left[ \ln \left( \frac{x}{L} \right) + \frac{L-x}{x_0} \right] - Fx & L - x_0 \leq x \leq L, \end{cases} \quad (1)$$

where  $a$  and  $x_0$  are the energy and the length scale factors which determine the height and the width of the well. The resulting potential is shown in Fig. 3. Such a potential well

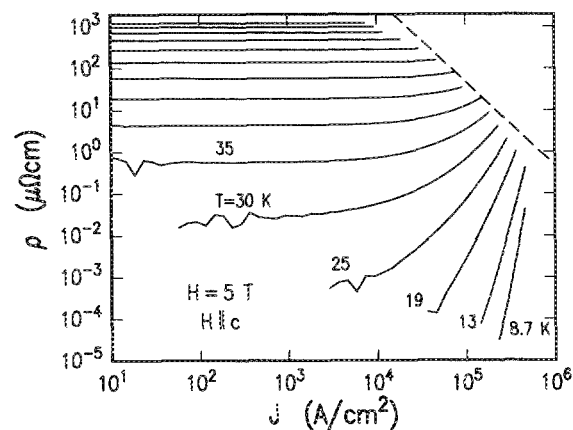


FIG. 2. Experimental  $\rho$ - $J$  characteristics at various temperatures at  $H = 5$  T. The high-temperature curves (35–80 K) are shown at 5 K intervals. The dashed line in the upper right corner is the limit of 1 mW power dissipation in the film, above which the measurements were limited by the self-heating effects.

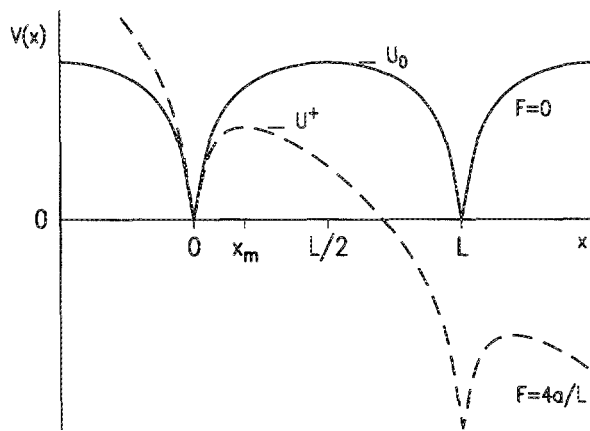


FIG. 3. Shape of the logarithmic potential well of Eq. (1) in absence (solid) and presence (dashed) of the driving force.

may arise from a localized defect that reduces the order parameter within a volume of a length scale on the order of the coherence length  $\xi$ . Since in high  $T_c$  materials  $\xi$  is only several angstroms, the well is expected to have a narrow conical structure. On the other hand, since the penetration depth  $\lambda$  is much larger than  $\xi$ , the magnetic field of an isolated vortex has a rather extended logarithmic decay which could account for the logarithmic broadening of the potential well. The distance  $L$  between the wells is the average distance between the defects in the case of an isolated vortex, or the Abrikosov flux lattice spacing  $a_0$  in the case of low defect density and flux bundle hopping.

The flux creep induced resistivity is determined by the net hopping rate in the direction of the driving force:

$$\rho = (v_0 B L / J) [\exp(-U^+ / kT) - \exp(-U^- / kT)], \quad (2)$$

where  $v_0$  is the attempt frequency and  $U^+$  and  $U^-$  are the barrier heights in the positive and negative direction, respectively. In the case of the logarithmic potential of Eq. (1) the following analytical solution is obtained:

$$x_m = \frac{L}{2} \left\{ \frac{F_0}{F} + 1 - \left[ \left( \frac{F_0}{F} \right)^2 + 1 \right]^{1/2} \right\} \quad x_0 \leq x_m \leq L/2$$

$$U^+ = a \ln \left( \frac{x_m(L-x_m)}{x_0 L} \right) + a - Fx_m \quad (3)$$

$$U^- = U^+ + FL,$$

where  $x_m$  is the driving force dependent position of the maximum of the potential and  $F_0 = 2a/L$ .

The resulting theoretical  $\rho$ - $J$  characteristics are shown in Fig. 4. At very low driving forces,  $F \ll F_0$  and  $FL < kT$ ,  $x_m$  is fixed at  $L/2$ , and  $U^\pm = U_0 \mp FL/2$  with  $U_0 = a[\ln(L/4x_0) + 1]$ . This is the regime in which  $\rho$  is independent of the Lorentz force  $F = JB V_c$ , where  $V_c$  is a correlation volume of the flux bundle:

$$\rho = (v_0 B^2 L^2 V_c / kT) \exp(-U_0 / kT). \quad (4)$$

On the other hand, for  $F \gg F_0$  (and  $FL > kT$ ) the potential well is distorted and  $x_m = a/F$  ( $x_m \ll L/2$ ) shifts with  $F$  so that the activation energy drops logarithmically with the

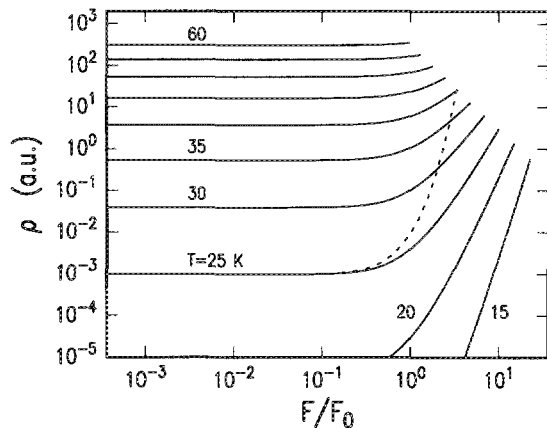


FIG. 4. Theoretical  $\rho$ - $J$  characteristics from Eqs. (2) and (3) at various temperatures. The parameters of the logarithmic potential well are  $U_0 = 50$  meV and  $L/x_0 = 200$ . The dotted curve, for comparison, shows the result of a sinusoidal potential well with the same  $U_0$ .

driving force,  $U^+ = a \ln(a/x_0 F)$ . In this regime, the  $\rho$ - $J$  characteristics attain the following power law form:

$$\rho = (v_0 BL/J)(x_0 F/a)^{a/kT}. \quad (5)$$

Figure 4 is not an attempt to fit the data, but rather is a graphic representation of the proposed model. In this plot we used temperature-independent parameters, whereas the height and the width of the well are expected to vary with temperature and hence may cause a shift between the curves. In addition, the details of the curvature of the potential around  $L/2$  will dictate the broadening of the transition between the regions of the constant  $\rho$  and the power law behavior. The degree of the sharpness of the well (on the order of  $\xi$ ) at  $x = 0$  is probed only at extremely high  $F$  values which are not accessible experimentally, and the particular choice in Eq. (1) of the linear extrapolation to the origin for  $x < x_0$  was made to simplify the mathematical expressions.

The transition into a superconducting vortex-glass phase<sup>5</sup> was recently suggested to explain the power law  $V$ - $I$  characteristics in  $\text{YBa}_2\text{Cu}_3\text{O}_7$  epitaxial films.<sup>2</sup> In this model, in the vicinity of the glass transition temperature  $T_g(H)$ , the  $\rho$ - $J$  characteristics above  $T_g$  are expected to show a transition from constant  $\rho$  to a power law behavior, in qualitative agreement with our data. At  $T_g$  the theory predicts a straight power law behavior  $V \propto I^n$ , with  $n \approx 3$ , whereas at  $T < T_g$  a negative curvature in the  $\rho$ - $J$  dependence is expected. Figure 2 reveals that in the  $\text{Bi}_2\text{Sr}_2\text{CaCu}_2\text{O}_8$  films the vortex-glass transition, if indeed it exists, must occur at  $T_g < 8.7$  K since

all the curves at higher temperatures show a positive curvature. However, at this temperature we obtain a value for  $n$  in excess of 12, which is inconceivable within the vortex-glass theory. In addition, the observation of the nonlinear behavior at temperatures high above the glass transition,  $(T - T_g)/T_g \gg 1$ , is inconsistent with the model as well. This clearly indicates that the power law behavior in  $\text{Bi}_2\text{Sr}_2\text{CaCu}_2\text{O}_8$  films is not related to a vortex-glass transition. Therefore, this theory appears not to constitute a general explanation for the power law  $V$ - $I$  characteristics in high  $T_c$  superconductors.

In conclusion, we have shown that the power law  $\rho$ - $J$  characteristics in high  $T_c$  epitaxial films, in the presence of magnetic field, are consistent with the flux creep model once the appropriate logarithmic flux line potential well structure is taken into account.

<sup>1</sup>M. Sugahara, M. Kojima, N. Yoshikawa, T. Akeyoshi, and N. Haneji, Phys. Lett. A **125**, 429 (1987); P. C. E. Stamp, L. Forro, and C. Ayache, Phys. Rev. B **38**, 2847 (1988); N. C. Yeh and C. C. Tsuei, Phys. Rev. B **39**, 9708 (1989); T. Onogi, T. Ichiguchi, and T. Aida, Solid State Commun. **69**, 991 (1989); D. H. Kim, A. M. Goldman, J. H. Kang, and R. T. Kampwirth, Phys. Rev. B **40**, 8834 (1989).

<sup>2</sup>R. H. Koch, V. Foglietti, W. J. Gallagher, G. Koren, A. Gupta, and M. P. A. Fisher, Phys. Rev. Lett. **63**, 1511 (1989).

<sup>3</sup>E. Zeldov, N. M. Amer, G. Koren, A. Gupta, M. W. McElfresh, and R. J. Gambino, Appl. Phys. Lett. **56**, 680 (1990).

<sup>4</sup>J. M. Kosterlitz and D. J. Thouless, J. Phys. C **6**, 1181 (1973); Prog. Low Temp. Phys. B **7**, 373 (1978).

<sup>5</sup>M. P. A. Fisher, Phys. Rev. Lett. **62**, 1415 (1989).

<sup>6</sup>A. Gupta, G. Koren, G. V. Chandrasekhar, and A. Segmüller, Proc. SPIE Symp. Microelectronic Integrated Processing: High  $T_c$  Superconductivity, Santa Clara, Oct. 1989 (to be published); G. Koren, A. Gupta, E. A. Giess, A. Segmüller, and R. B. Laibowitz, Appl. Phys. Lett. **54**, 1054 (1989); G. Koren, A. Gupta, and R. J. Baseman, Appl. Phys. Lett. **54**, 1920 (1989).

<sup>7</sup>P. W. Anderson, Phys. Rev. Lett. **9**, 309 (1962); P. W. Anderson and Y. B. Kim, Rev. Mod. Phys. **36**, 39 (1964); M. Tinkham, Introduction to Superconductivity (McGraw-Hill, New York, 1975).

<sup>8</sup>M. Tinkham, Phys. Rev. Lett. **61**, 1658 (1988).

<sup>9</sup>E. Zeldov, N. M. Amer, G. Koren, A. Gupta, R. J. Gambino, and M. W. McElfresh, Phys. Rev. Lett. **62**, 3093 (1989); E. Zeldov, N. M. Amer, and G. Koren, Physica C **162-164**, 1599 (1989).

<sup>10</sup>Y. Yeshurun and A. P. Malozemoff, Phys. Rev. Lett. **60**, 2202 (1988); Y. Yeshurun, A. P. Malozemoff, T. K. Worthington, R. M. Yandrofski, L. Krusin-Elbaum, F. Holtzberg, T. R. Dinger, and G. V. Chandrasekhar, Cryogenics **29**, 258 (1989).

<sup>11</sup>T. T. M. Palstra, B. Batlogg, L. F. Schneemeyer, and J. V. Waszczak, Phys. Rev. Lett. **61**, 1662 (1988); T. T. M. Palstra, B. Batlogg, R. B. van Dover, L. F. Schneemeyer, and J. V. Waszczak, Appl. Phys. Lett. **54**, 763 (1989).

<sup>12</sup>A. P. Malozemoff, T. K. Worthington, E. Zeldov, N. C. Yeh, M. W. McElfresh, and F. Holtzberg, in Springer Series in Physics, Strong Correlations and Superconductivity, edited by H. Fukuyama, S. Maekawa, and A. P. Malozemoff (Springer, Heidelberg, 1989), p. 349.